Geomechanics and Engineering, *Vol. 38, No. 4 (2024) 409-420*
https://doi.org/10.12989/gae.2024.38.4.409

Analysis of the hygro-thermo-mechanical response of functionally graded plates resting on elastic foundations based on various micromechanical models

Belkacem Adim*[1,2] and Tahar Hassaine Daouadji[2,3]

[1]*Department of Sciences and technology, Tissemsilt University, Tissemsilt, Algeria*
[2]*Geomatics and Sustainable Development Laboratory, Ibn Khaldoun University, Tiaret, Algeria*
[3]*Department of Civil engineering, Ibn Khaldoun University, Tiaret, Algeria*

(*Received May 6, 2024, Revised August 12, 2024, Accepted August 13, 2024*)

Abstract. In this research the hygro-thermo-mechanical loading and micromechanical model effects on bending behavior of functionally graded material plates resting on Winkler and Pasternak elastic foundations, the higher order shear deformation theory is used here. The material properties of the plate: young's modulus, thermal coefficient and moisture expansion coefficient are assumed to be graded in the thickness direction according to various micromechanical models starting with the Voigt's model which is commonly used in most functionally graded plates studies to the Reuss's, LRVE's and Mori-Tanaka's models. The principle of virtual displacement is used to determine the equilibrium equations and the a several numerical results are given to validate the precision of the present method for bending behavior of FGM plates subjected to hygro-thermo-mechanical loading resting on elastic foundations. Afterwards, a parametric study is conducted to determine the effect of different parameters on the deflection of the FGM plates like micromechanical models, type of loading and plate geometry. In the lights of the present research, it can be concluded that the present theory is accurate and simple in predicting the deflection behavior of functionally graded plates under hygro-thermo-mechanical effects and micromechanical models.

Keywords: deflection; elastic foundations; functionally graded plates; hygro-thermo-mechanical loading; micromechanical models

1. Introduction

The concept of functionally graded materials (FGMs) was the first introduced in 1984 by a group of material scientists in Japan, as ultrahigh temperature resistant materials for aircraft, space vehicles and other engineering applications. Functionally graded materials (FGMs) are new composite materials in which the micro-structural details are spatially varied through non-uniform distribution of the reinforcement phase. This is achieved by using reinforcement with different properties, sizes and shapes, as well as by interchanging the role of reinforcement and matrix phase in a continuous manner. The result is a microstructure that produces continuous or smooth change on thermal and mechanical properties at the macroscopic or continuum level. Now, FGMs are developed for general use as structural components in extremely high temperature environments. The functionally graded materials are used in several high-tech structural applications, but their performance significantly decreases in the long term due to moisture concentration and high temperatures. consequently, environmental effects (temperature and humidity) cause hygrothermal stresses in the FGM structures, which leads to a significant deformation and might even cause the breakdown of the structure. The effect of moisture and temperature on the deformation and stress of different FGM structures has been studied over the years by many researchers (Sharma and Singh 2019, Bagheri *et al.* 2021, Shariyat *et al*. 2019, Tounsi *et al.* 2023, Sobhy 2016).

Over the years, the mechanics of structures in its broad concept have attracted the attention of many researchers and experts in the field (Gao *et al.* 2022, Liu *et al.* 2022, Wang and Sigmund 2023, Zhang *et al.* 2023, Zhang *et al.* 2024, Cao *et al.* 2024).

In the literature, we can find numerous studies on structures supported by elastic foundations. Kaddari *et al.* (2020), Kiani *et al.* (2014), Hachemi *et al.* (2017), Daouadji *et al.* (2016) presented a study on the structural behavior of perfect and porous FGM plates resting on elastic foundations. Nguyen *et al.* (2023) examined the mechanical behavior of functionally graded beams resting on elastic foundations using the Legendre-Ritz solution. Gupta *et al.* (2016a) used the finite element method to determine the natural frequency of FGM plates resting on elastic foundations; Soltani *et al.* (2019) and Parida *et al.* (2018) investigated the buckling and the free vibration behavior of the FGM plates supported by elastic foundations. Many studies have been conducted to examine the behavior of functionally graded shells, beams, and plates subjected to mechanical, thermal, or thermo-mechanical loading. Sadowski *et al.* (2015) presented a comparison between

*Corresponding author, Professor
E-mail: adim.belkacem@univ-tissemsilt.dz

ISSN: 2005-307X (Print), 2092-6219 (Online)

finite elements and analytical models when examining the behavior of multilayered and FGM structural elements subjected to mechanical and thermal loads. Reddy (2000) considered the impact of the third-order shear deformation theory (THSDT) on FGM plates under mechanical loading. Bagheri *et al.* (2021), Bagheri *et al.* (2023), Ghiasian *et al.* (2013) studied the thermally induced nonlinear vibration of FGM-jointed conical-conical shells. Another study by Amari and Maktoof (2023) suggested another method to examine the thermoelastic behavior of cylindrical sandwich shells with axially graded graphene-plate-reinforced composite (AG-GPLRC) face sheets and a core made of polymer. Daouadji and Adim (2016), Mudhaffar *et al.* (2021), Kiani *et al.* (2015), Kiani *et al.* (2013), Kitipornchai *et al.* (2006), Daouadji *et al.* (2016), presented the bending, buckling and free vibration behavior analysis of FGM plates under different types of loading using quasi-three-dimensional and two-dimensional higher-order shear deformation theories.

Since the concept of FGM structures eliminate the material's discontinuity problem through the thickness, FGM material properties are assumed to vary continuously and gradually across the thickness. Several researchers focused their works on the material's properties variation of FGM structures. Gasik (1998) examined a wide range of micromechanical modelling approaches for the elastic and elastoplastic computation of Tungsten/Copper functionally graded plate. Zhang *et al.* (2020) suggested a micromechanics-based algorithm to study the elastoplastic behavior of functionally graded material. Nemati and Mahmoodabadi (2020) considered Eight types of micromechanical models in investigating the buckling behavior of FGM thin conical panels exposed to thermal environments and surrounded by elastic foundation using analytical approach. Zaidi *et al.* (2021) presented a review of the various modelling techniques used for the determination of the variable material properties of FGM plates and their analysis. Shahsavari and Karami (2022) gave an assessment of the Reuss, Tamura, and LRVE models on vibration behavior of FG nanoplates. From this bibliographic review, we found out that it is uncommon to find comprehensive research addressing the various aspects of the behavior of functionally graded plates concurrently, particularly when it comes to the investigation of the impact of the micromechanical model selection on the flexural behavior of FGM plates supported by elastic foundations and subjected to hygro, thermo, mechanical, or a combination of two to three of these previous loadings.

The primary objective of this paper is to present a general formulation for functionally graded plates (FGP) using a new higher order shear deformation plate theory with only four unknown functions, it is indeed the refined four variables high order theory to investigate the impact of micromechanical models on the hygro-thermo-mechanical flexural behavior of functionally graded plates resting on elastic foundations. The present theory satisfies equilibrium conditions at the top and bottom faces of the plate without using shear correction factors. The hyperbolic function in terms of thickness coordinate is used in the displacement field to account for shear deformation. Governing equations are derived from the principle of minimum total potential energy. Navier solution is used to obtain the closed-form solutions for simply supported FG plates. This study will provide insights into the behavior of FGM structures under different loading conditions and contribute to the understanding and design of FGM materials for various applications. In this study, a new displacement models for an analysis of the hygro-thermo-mechanical loading and micromechanical model effects on bending behavior of functionally graded material plates resting on Winkler and Pasternak elastic foundations, the higher order shear deformation theory is used here are proposed. The plates are made of an isotropic material with material properties varying in the thickness direction only. let us cite as an example: Young's modulus, thermal coefficient and moisture expansion coefficient are assumed to be graded in the thickness direction according to various micromechanical models starting with the Voigt's model which is commonly used in most functionally graded plates studies to the Reuss's, LRVE's and Mori-Tanaka's models. Analytical solutions for bending deflections of FGM plates are obtained. Based on the principle of virtual displacement is used to determine the equilibrium equations and several numerical results are given to validate the precision of the present method for bending behavior of FGM plates subjected to hygro-thermo-mechanical loading resting on elastic foundations. Afterwards, a parametric study is conducted to determine the effect of different parameters on the deflection of the FGM plates like micromechanical models, type of loading and plate geometry. Numerical examples are presented to illustrate the accuracy and efficiency of the present theory by comparing the obtained results with those computed using various other theories. We can say that in the light of the present results obtained, that the present theory is accurate and simple in predicting the deflection behavior of functionally graded plates under hygro-thermo-mechanical effects and micromechanical models.

2. FGM micromechanical models

In this study we consider a functionally graded material plate of dimensions (length a, width b and thickness h). The plate materials properties are varying continuously from metal in the bottom to ceramic in the top face. The plate is subjected to a combination of loads: mechanical load $q(x,y)$ and a temperature field $T(x, y, z)$ also a moisture concentration $C(x, y, z)$. The effective material properties $V(z)$ of the FGM plate, such as Young's modulus E, Poisson's ratio ν, and thermal α and moisture expansion βcoefficients are given according to different micromechanical models.

Where V_c and V_m are the corresponding properties of the ceramic and metal, respectively, and p is the volume fraction exponent which takes values from zero in the case of ceramic to infinity in the case of metal.

2.1 Voigt micromechanical model

The simplest micromechanical model is Voigt's model, this why it is used often in almost all FGM studies. The effective properties are given by this model in Eq. (1) as follows: (Gasik 1998)

$$V(z) = V_m + (V_c - V_m)(\frac{1}{2} + \frac{z}{h})^p \tag{1}$$

2.2 Reuss micromechanical model

Reuss posited the uniformity of the stress across the material and achieved the effective properties given by Akbarzadeh *et al.* (2015) in Eq. (2) as follows

$$V(z) = \frac{V_c V_m}{V_c(1-(\frac{1}{2} + \frac{z}{h})^p) + V_m(\frac{1}{2} + \frac{z}{h})^p} \tag{2}$$

2.3 LRVE micromechanical model

The LRVE (local cubic representative volume elements) model was used by Gasik (1998) to determine the FGM's effective material properties. Following the LRVE micromechanical model, the material properties are presented in Eq. (3) by

$$V(z) = V_m(1 + \frac{(\frac{1}{2} + \frac{z}{h})^p}{\frac{1}{1-\frac{V_m}{V_c}} - (\frac{1}{2} + \frac{z}{h})^{\frac{p}{3}}}) \tag{3}$$

2.4 Mori-Tanaka micromechanical model

Micromechanical models like the Mori-Tanaka model may be used to obtain the locally effective material properties (Mori and Tanaka 1973). According to this approach, the heterogeneous material is a two-phase composite made up of a matrix reinforced by spherical particles that are dispersed at random over the plate. The Mori-Tanaka homogenization scheme states that the material properties are represented in Eq. (4) by Zuiker (1995) as fellow

$$V(z) = V_m + (V_c - V_m)(\frac{(\frac{1}{2} + \frac{z}{h})^p}{1 + (1-(\frac{1}{2} + \frac{z}{h})^p)(\frac{V_c}{V_m} - 1)\frac{(1+\nu)}{(3-3\nu)}}) \tag{4}$$

3. Mathematical formulation of the present model

Considering a plate made of a functionally graded material throughout its thickness "h" (Fig. 1). The material is considered to be isotropic and graduated along its thickness The "z" axis is upward positive from the mid plane and the "xy" plane is assumed to represent the plate's undeformed mid plane.

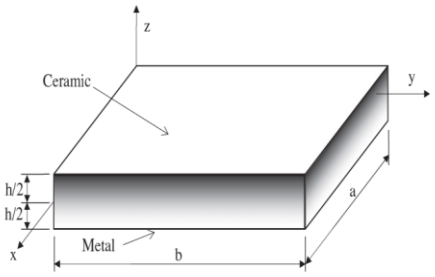

Fig. 1 Geometry of a rectangular FGM plate

3.1 Cinematics and strains

The displacement field for the present model is considered by Eq. (5(a)) as follows

$$\begin{aligned} u(x,y,z) &= u_0(x,y) - z\frac{\partial w_b}{\partial x} - \left(z - h\sinh\left(\frac{z}{h}\right) + z\cosh\left(\frac{1}{2}\right)\right)\frac{\partial w_s}{\partial x} \\ v(x,y,z) &= v_0(x,y) - z\frac{\partial w_b}{\partial y} - \left(z - h\sinh\left(\frac{z}{h}\right) + z\cosh\left(\frac{1}{2}\right)\right)\frac{\partial w_s}{\partial y} \\ w(x,y,z) &= w_b(x,y) + w_s(x,y) \end{aligned} \tag{5a}$$

where the displacements in the mid-plane of the FGM plate u_0 and v_0 are in the x and y direction, respectively; the bending w_b and shear w_s components of transverse displacement (Adim *et al.*2016), while the form functions that determinate the transversal shear stresses and strains distribution of through the plate's thickness is expressed in Eq. (5(b)) as follows

$$f(z) = z - h\sinh\left(\frac{z}{h}\right) + z\cosh\left(\frac{1}{2}\right) \tag{5b}$$

By derivation of the displacement field, the strains relations can be given in Eqs. (6(a)) and (6(b)) by

$$\begin{aligned} \varepsilon_x &= \frac{\partial u_0}{\partial x} - z\frac{\partial^2 w_b}{\partial x^2} - f(z)\frac{\partial^2 w_s}{\partial x^2} \\ \varepsilon_y &= \frac{\partial v_0}{\partial y} - z\frac{\partial^2 w_b}{\partial y^2} - f(z)\frac{\partial^2 w_s}{\partial y^2} \\ \gamma_{xy} &= \frac{\partial u_0}{\partial y} + \frac{\partial v_0}{\partial x} - 2z\frac{\partial^2 w_b}{\partial x\partial y} - 2f(z)\frac{\partial^2 w_s}{\partial x\partial y} \\ \gamma_{yz} &= g(z)\frac{\partial w_s}{\partial y} \\ \gamma_{xz} &= g(z)\frac{\partial w_s}{\partial x} \\ \varepsilon_z &= 0 \end{aligned} \tag{6a}$$

Knowing that

$$\begin{aligned} &\varepsilon_x^0 = \frac{\partial u_0}{\partial x},\ k_x^b = -\frac{\partial^2 w_b}{\partial x^2},\ k_x^s = -\frac{\partial^2 w_s}{\partial x^2},\ \varepsilon_y^0 = \frac{\partial v_0}{\partial y}, \\ &k_y^b = -\frac{\partial^2 w_b}{\partial y^2},\ k_y^s = -\frac{\partial^2 w_s}{\partial y^2}),\ \gamma_{xy}^0 = \frac{\partial u_0}{\partial y} + \frac{\partial v_0}{\partial x}, \\ &k_{xy}^b = -2\frac{\partial^2 w_b}{\partial x\partial y},\ k_{xy}^s = -2\frac{\partial^2 w_s}{\partial x\partial y},\ \gamma_{yz}^s = \frac{\partial w_s}{\partial y},\ \gamma_{xz}^s = \frac{\partial w_s}{\partial x}, \\ &g(z) = 1 - f'(z) \text{ and } f'(z) = \frac{df(z)}{dz} \end{aligned} \tag{6b}$$

The strains are shown in Eq. (6(c)) by

$$\begin{aligned}\varepsilon_x &= \varepsilon_x^0 + z\,k_x^b + f(z)\,k_x^s\\ \varepsilon_y &= \varepsilon_y^0 + z\,k_y^b + f(z)\,k_y^s\\ \gamma_{xy} &= \gamma_{xy}^0 + z\,k_{xy}^b + f(z)\,k_{xy}^s\\ \gamma_{yz} &= g(z)\,\gamma_{yz}^s\\ \gamma_{xz} &= g(z)\,\gamma_{xz}^s\\ \varepsilon_z &= 0\end{aligned} \tag{6c}$$

3.2 Constitutive equations

The relation stress-strain is expressed in Eq. (7) by

$$\begin{Bmatrix}\sigma_x\\ \sigma_y\\ \tau_{xy}\end{Bmatrix} = \begin{bmatrix}Q_{11} & Q_{12} & 0\\ Q_{12} & Q_{22} & 0\\ 0 & 0 & Q_{66}\end{bmatrix}\begin{Bmatrix}\varepsilon_x - \alpha\Delta T - \beta\Delta C\\ \varepsilon_y - \alpha\Delta T - \beta\Delta C\\ \gamma_{xy}\end{Bmatrix},\qquad \begin{Bmatrix}\tau_{yz}\\ \tau_{xz}\end{Bmatrix} = \begin{bmatrix}Q_{44} & 0\\ 0 & Q_{55}\end{bmatrix}\begin{Bmatrix}\gamma_{yz}\\ \gamma_{xz}\end{Bmatrix} \tag{7}$$

Where $(\varepsilon_x, \varepsilon_y, \gamma_{xy}, \gamma_{yz}, \gamma_{xz})$ and $(\sigma_x, \sigma_y, \tau_{xy}, \tau_{yz}, \tau_{xz})$ are the deformations and normal/shear stresses components, respectively. Using the material properties exhibited in Eqs. (1)-(4), stiffness coefficients, Q_{ij}, can be given in Eq. (8) as

$$Q_{11} = Q_{22} = \frac{E(z)}{1-\nu^2},\ Q_{12} = \frac{\nu E(z)}{1-\nu^2},\qquad Q_{44} = Q_{55} = Q_{66} = \frac{E(z)}{2(1+\nu)} \tag{8}$$

Where $\Delta C = C - C_0$ and $\Delta T = T - T_0$ in which C_0 is the moisture concentration of reference and T_0 is the temperature of reference.

Assuming the distribution of temperature "T" and the concentration of moisture "C" in the volume of the plate area are described in Eq. (9) as fellows

$$\begin{aligned}T(x,y,z) &= T_z(z)\,T_A(x,y),\\ C(x,y,z) &= C_z(z)\,C_A(x,y)\end{aligned} \tag{9}$$

Knowing that $T_z(z)$ and $C_z(z)$ represent the concentration profile of the temperature and the moisture in direction of the plate thickness "z", respectively, while $T_A(x, y)$ and $C_A(x, y)$ are the concentration of the temperature and the moisture distributions over the reference section "A".

In the present research, the temperature distribution field "T" and the moisture concentration "C" are written in Eq. (10) by Mudhaffar *et al.* (2021) as fellows

$$\begin{aligned}T(x,y,z) &= T_1(x,y) + \frac{z}{h}T_2(x,y) + \frac{1}{\pi}\sin\left(\frac{\pi z}{h}\right)T_3(x,y)\\ C(x,y,z) &= C_1(x,y) + \frac{z}{h}C_2(x,y) + \frac{1}{\pi}\sin\left(\frac{\pi z}{h}\right)C_3(x,y)\end{aligned} \tag{10}$$

3.3 Equilibrium equations

The equilibrium equations can be obtained using the virtual work's principle. The virtual displacements principle is defined in Eq. (11) by

$$\int_V \sigma_{ij}\delta\varepsilon_{ij}dV - \int_A (q - f_e)\delta w\,dA = 0 \tag{11}$$

Where "A" is the top surface and "$\mathbf{f_e}$ "is the reaction of the elastic foundation given by Eq. (12) as fellow

$$f_e = K_w w - J_1\frac{\partial w}{\partial x^2} - J_2\frac{\partial w}{\partial y^2} \tag{12}$$

where K_w is the elastic modulus of the foundation and J_1 and J_2 are the shear moduli of the foundation. If the foundation is isotropic and homogeneous, this means that $J_1=J_2=J_0$. If the shear moduli of the foundation are neglected, Pasternak foundation becomes a Winkler foundation.

Replacing Eqs. (6) and (7) into Eq. (11) and integrating along the plate's thickness, Eq. (11) will be presented in the form of Eq. (13) by

$$\begin{aligned}&\int_A [N_x\delta\varepsilon_x^0 + N_y\delta\varepsilon_y^0 + N_{xy}\delta\gamma_{xy}^0 + M_x^b\delta k_x^b\\ &+M_y^b\delta k_y^b + M_{xy}^b\delta k_{xy}^b + M_x^s\delta k_x^s + M_y^s\delta k_y^s\\ &+M_{xy}^s\delta k_{xy}^s + Q_{xz}^s\delta\gamma_{xz}^s + Q_{yz}^s\delta\gamma_{yz}^s]dA\\ &-\int_A (q - f_e)(\delta w_b + \delta w_s)dA = 0\end{aligned} \tag{13}$$

Where the stress resultants N, M, and Q^s are detailed in Eqs. (14(a)) and (14(b)) as

$$\begin{Bmatrix}N_x\\ N_y\\ N_{xy}\\ M_x^b\\ M_y^b\\ M_{xy}^b\\ M_x^s\\ M_y^s\\ M_{xy}^s\end{Bmatrix} = \int_{-h/2}^{h/2}\begin{Bmatrix}\sigma_x\\ \sigma_y\\ \tau_{xy}\\ z\sigma_x\\ z\sigma_y\\ z\tau_{xy}\\ f(z)\sigma_x\\ f(z)\sigma_y\\ f(z)\tau_{xy}\end{Bmatrix}dz = \begin{bmatrix}A_{11} & A_{12} & 0 & B_{11} & B_{12} & 0 & B_{11}^s & B_{12}^s & 0\\ A_{12} & A_{22} & 0 & B_{12} & B_{22} & 0 & B_{12}^s & B_{22}^s & 0\\ 0 & 0 & A_{66} & 0 & 0 & B_{66} & 0 & 0 & B_{66}^s\\ B_{11} & B_{12} & 0 & D_{11} & D_{12} & 0 & D_{11}^s & D_{12}^s & 0\\ B_{12} & B_{22} & 0 & D_{12} & D_{22} & 0 & D_{12}^s & D_{22}^s & 0\\ 0 & 0 & B_{66} & 0 & 0 & D_{66} & 0 & 0 & D_{66}^s\\ B_{11}^s & B_{12}^s & 0 & D_{11}^s & D_{12}^s & 0 & H_{11}^s & H_{12}^s & 0\\ B_{12}^s & B_{22}^s & 0 & D_{12}^s & D_{22}^s & 0 & H_{12}^s & H_{22}^s & 0\\ 0 & 0 & B_{66}^s & 0 & 0 & D_{66}^s & 0 & 0 & H_{66}^s\end{bmatrix}\begin{Bmatrix}\varepsilon_x^0\\ \varepsilon_y^0\\ \gamma_{xy}^0\\ k_x^b\\ k_y^b\\ k_{xy}^b\\ k_x^s\\ k_y^s\\ k_{xy}^s\end{Bmatrix} - \begin{Bmatrix}N_x^T\\ N_y^T\\ 0\\ M_x^{bT}\\ M_y^{bT}\\ 0\\ M_x^{sT}\\ M_y^{sT}\\ 0\end{Bmatrix} - \begin{Bmatrix}N_x^C\\ N_y^C\\ 0\\ M_x^{bC}\\ M_y^{bC}\\ 0\\ M_x^{sC}\\ M_y^{sC}\\ 0\end{Bmatrix} \tag{14a}$$

$$\begin{Bmatrix}Q_{yz}^s\\ Q_{xz}^s\end{Bmatrix} = \int_{-h/2}^{h/2} g(z)\begin{Bmatrix}\tau_{yz}\\ \tau_{yz}\end{Bmatrix}dz = \begin{bmatrix}A_{44}^s & 0\\ 0 & A_{55}^s\end{bmatrix}\begin{Bmatrix}\gamma_{yz}^s\\ \gamma_{xz}^s\end{Bmatrix} \tag{14b}$$

Where A_{ij} , B_{ij} , D_{ij} etc., are the stiffness of the plate, defined in Eqs. (15(a))-(15(c)) as

$$\begin{Bmatrix}A_{11} & B_{11} & D_{11} & B_{11}^s & D_{11}^s & H_{11}^s\\ A_{12} & B_{12} & D_{12} & B_{12}^s & D_{12}^s & H_{12}^s\\ A_{66} & B_{66} & D_{66} & B_{66}^s & D_{66}^s & H_{66}^s\end{Bmatrix} = \int_{-h/2}^{h/2}(1, z, z^2, f(z), z\,f(z), f^2(z))\begin{Bmatrix}Q_{11}\\ Q_{12}\\ Q_{66}\end{Bmatrix}dz \tag{15a}$$

$$(A_{22}, B_{22}, D_{22}, B_{22}^s, D_{22}^s, H_{22}^s) = (A_{11}, B_{11}, D_{11}, B_{11}^s, D_{11}^s, H_{11}^s) \tag{15b}$$

$$A^s_{44} = \int_{-h/2}^{h/2} Q_{44}\left(g(z)\right)^2 dz$$
$$A^s_{55} = \int_{-h/2}^{h/2} Q_{55}\left(g(z)\right)^2 dz \quad (15c)$$

The stress and moment resultants due to the hygrothermal loading $N^T_x = N^T_y$, $M^{bT}_x = M^{bT}_y$, $M^{sT}_x = M^{sT}_y$, $N^C_x = N^C_y$, $M^{bC}_x = M^{bC}_y$, $M^{sC}_x = M^{sC}_y$ are given in Eqs. (16(a)) and (16(b)) as fellow

$$\begin{Bmatrix} N^T_x \\ M^{bT}_x \\ M^{sT}_x \end{Bmatrix} = \int_{-h/2}^{h/2} \frac{E(z)}{1-\nu}\alpha(z)T \begin{Bmatrix} 1 \\ z \\ f(z) \end{Bmatrix} dz \quad (16a)$$

$$\begin{Bmatrix} N^C_x \\ M^{bC}_x \\ M^{sC}_x \end{Bmatrix} = \int_{-h/2}^{h/2} \frac{E(z)}{1-\nu}\beta(z)C \begin{Bmatrix} 1 \\ z \\ f(z) \end{Bmatrix} \quad (16b)$$

The equilibrium equations can be derived from Eq. (11) by integrating the displacement partially and considering the coefficients δu_0, δv_0, δw_b and δw_s null separately. From where the equilibrium equations related to the present refined theory can be presented in Eq. (17) as

$$\begin{aligned}
&\delta u_0: \quad \frac{\partial N_x}{\partial x} + \frac{\partial N_{xy}}{\partial y} = 0 \\
&\delta v_0: \quad \frac{\partial N_{xy}}{\partial x} + \frac{\partial N_y}{\partial y} = 0 \\
&\delta w_b: \quad \frac{\partial^2 M^b_x}{\partial x^2} + 2\frac{\partial^2 M^b_{xy}}{\partial x \partial y} + \frac{\partial^2 M^b_y}{\partial y^2} - f_e + q = 0 \\
&\delta w_s: \quad \frac{\partial^2 M^s_x}{\partial x^2} + 2\frac{\partial^2 M^s_{xy}}{\partial x \partial y} + \frac{\partial^2 M^s_y}{\partial y^2} + \frac{\partial Q^s_{xz}}{\partial x} + \frac{\partial Q^s_{yz}}{\partial y} - f_e + q = 0
\end{aligned} \quad (17)$$

Substituting from Eq. (14) into Eq. (17), Eq. (17) can be presented in Eqs. (18(a))-(18(d)) as fellow

$$\begin{aligned}
&A_{11}\frac{\partial^2 u_0}{\partial x^2} + A_{66}\frac{\partial^2 u_0}{\partial y^2} + (A_{12}+A_{66})\frac{\partial^2 v_0}{\partial x \partial y} - B_{11}\frac{\partial^3 w_b}{\partial x^3} \\
&-(B_{12}+2B_{66})\frac{\partial^3 w_b}{\partial x \partial y^2} - (B^s_{12}+2B^s_{66})\frac{\partial^3 w_s}{\partial x \partial y^2} - B^s_{11}\frac{\partial^3 w_s}{\partial x^3} = f_1
\end{aligned} \quad (18a)$$

$$\begin{aligned}
&A_{22}\frac{\partial^2 v_0}{\partial y^2} + A_{66}\frac{\partial^2 v_0}{\partial x^2} + (A_{12}+A_{66})\frac{\partial^2 u_0}{\partial x \partial y} - B_{22}\frac{\partial^3 w_b}{\partial y^3} \\
&-(B_{12}+2B_{66})\frac{\partial^3 w_b}{\partial x^2 \partial y} - (B^s_{12}+2B^s_{66})\frac{\partial^3 w_s}{\partial x^2 \partial y} - B^s_{22}\frac{\partial^3 w_s}{\partial y^3} = f_2
\end{aligned} \quad (18b)$$

$$\begin{aligned}
&B_{11}\frac{\partial^3 u_0}{\partial x^3} + (B_{12}+2B_{66})\frac{\partial^3 u_0}{\partial x \partial y^2} + (B_{12}+2B_{66})\frac{\partial^3 v_0}{\partial x^2 \partial y} + B_{22}\frac{\partial^3 v_0}{\partial y^3} \\
&-D_{11}\frac{\partial^4 w_b}{\partial x^4} - 2(D_{12}+2D_{66})\frac{\partial^4 w_b}{\partial x^2 \partial y^2} - D_{22}\frac{\partial^4 w_b}{\partial y^4} \\
&-D^s_{11}\frac{\partial^4 w_s}{\partial x^4} - 2(D^s_{12}+2D^s_{66})\frac{\partial^4 w_s}{\partial x^2 \partial y^2} - D^s_{22}\frac{\partial^4 w_s}{\partial y^4} = f_3
\end{aligned} \quad (18c)$$

$$\begin{aligned}
&B^s_{11}\frac{\partial^3 u_0}{\partial x^3} + (B^s_{12}+2B^s_{66})\frac{\partial^3 u_0}{\partial x \partial y^2} + (B^s_{12}+2B^s_{66})\frac{\partial^3 v_0}{\partial x^2 \partial y} + B^s_{22}\frac{\partial^3 v_0}{\partial y^3} \\
&-D^s_{11}\frac{\partial^4 w_b}{\partial x^4} - 2(D^s_{12}+2D^s_{66})\frac{\partial^4 w_b}{\partial x^2 \partial y^2} - D^s_{22}\frac{\partial^4 w_b}{\partial y^4} - H^s_{11}\frac{\partial^4 w_s}{\partial x^4} \\
&-2(H^s_{12}+2H^s_{66})\frac{\partial^4 w_s}{\partial x^2 \partial y^2} - H^s_{22}\frac{\partial^4 w_s}{\partial y^4} + A^s_{55}\frac{\partial^2 w_s}{\partial x^2} + A^s_{44}\frac{\partial^2 w_s}{\partial y^2} = f_4
\end{aligned} \quad (18d)$$

Where $\{f\} = \{f_1, f_2, f_3, f_4\}^t$ is the vector of forces, where they are given in Eq. (19) as

$$\begin{aligned}
&f_1 = \frac{\partial N^T_x}{\partial x} + \frac{\partial N^C_x}{\partial x}, \quad f_2 = \frac{\partial N^T_y}{\partial y} + \frac{\partial N^C_y}{\partial y}, \\
&f_3 = f_e + q - \frac{\partial^2 (M^{bT}_x + M^{bC}_x)}{\partial x^2} - \frac{\partial^2 (M^{bT}_y + M^{bC}_y)}{\partial y^2}, \\
&f_4 = f_e + q - \frac{\partial^2 (M^{sT}_x + M^{sC}_x)}{\partial x^2} - \frac{\partial^2 (M^{sT}_y + M^{sC}_y)}{\partial y^2}
\end{aligned} \quad (19)$$

4. Precise solution of FGM plate

A double trigonometric series is used to represent the uniform external force, transverse uniform temperature, and moisture concentration loads according to the Navier technique. Here, we are interested in the precise solution of Eq. (18) for a simply supported functionally graded plate. In order to overcome this issue, Navier made the following assumptions defined in Eq. (20) for the transverse mechanical, hygro and thermal loads, q, T_i, and C_i:

$$\begin{aligned}
&q = q_0 \sin(\lambda x)\sin(\mu y) \\
&T_i = t_i \sin(\lambda x)\sin(\mu y) \quad \text{with} \quad (i = 1,2,3) \\
&C_i = c_i \sin(\lambda x)\sin(\mu y) \quad \text{with} \quad (i = 1,2,3)
\end{aligned} \quad (20)$$

Where $\lambda = \left(\frac{\pi}{a}\right)$, $\mu = \left(\frac{\pi}{b}\right)$. q_0, t_i and c_i are assumed constants and T_i and C_i are given in Eq. (10).

By applying the Navier's technique, we adopt the following solution for u_0, v_0, w_b and w_s that satisfies the boundary conditions of the plate

$$\begin{Bmatrix} u_0 \\ v_0 \\ w_b \\ w_s \end{Bmatrix} = \begin{Bmatrix} U\cos(\lambda x)\sin(\mu y) \\ V\sin(\lambda x)\cos(\mu y) \\ W_b \sin(\lambda x)\sin(\mu y) \\ W_s \sin(\lambda x)\sin(\mu y) \end{Bmatrix} \quad (21)$$

Where U, V, W_b and W_s are parameters that satisfying the solution of Eq. (21) and guaranteeing the resolution of Eq. (18). From where we obtain the equation's system as

$$\begin{bmatrix} s_{11} & s_{12} & s_{13} & s_{14} \\ s_{12} & s_{22} & s_{23} & s_{24} \\ s_{13} & s_{23} & s_{33} & s_{34} \\ s_{14} & s_{24} & s_{34} & s_{44} \end{bmatrix} \begin{Bmatrix} U \\ V \\ W_b \\ W_s \end{Bmatrix} = \begin{Bmatrix} F_1 \\ F_2 \\ F_3 \\ F_4 \end{Bmatrix} \quad (22)$$

Where

$$\begin{aligned}
&s_{11} = -(A_{11}\lambda^2 + A_{66}\mu^2), \\
&s_{12} = -\lambda\,\mu\,(A_{12} + A_{66}), \\
&s_{13} = \lambda\,[B_{11}\lambda^2 + (B_{12}+2B_{66})\,\mu^2], \\
&s_{22} = -(A_{66}\lambda^2 + A_{22}\mu^2), \\
&s_{14} = \lambda\,[B^s_{11}\lambda^2 + (B^s_{12}+2B^s_{66})\,\mu^2], \\
&s_{23} = \mu\,[(B_{12}+2B_{66})\,\lambda^2 + B_{22}\mu^2], \\
&s_{24} = \mu\,[(B^s_{12}+2B^s_{66})\,\lambda^2 + B^s_{22}\mu^2], \\
&s_{33} = -(D_{11}\lambda^4 + 2(D_{12}+2D_{66})\lambda^2\mu^2 \\
&\quad + D_{22}\mu^4 + K_w + J_1\lambda^2 + J_2\mu^2), \\
&s_{34} = -(D^s_{11}\lambda^4 + 2(D^s_{12}+2D^s_{66})\lambda^2\,\mu^2 \\
&\quad + D^s_{22}\,\mu^4 + K_w + J_1\lambda^2 + J_2\mu^2), \\
&s_{44} = -(H^s_{11}\lambda^4 + 2(H^s_{12}+2H^s_{66})\lambda^2\mu^2 + H^s_{22}\mu^4 + A^s_{55}\lambda^2 \\
&\quad + A^s_{44}\mu^2 + D^s_{22}\,\mu^4 + K_w + J_1\lambda^2 + J_2\mu^2)
\end{aligned} \quad (23)$$

The components of the force vector $\{F\}=\{F_1,F_2,F_3,F_4\}^t$ are written in Eqs. (24)-(26) as

$$\begin{aligned}
F_1 &= \lambda\left[(A^C c_1 + B^C c_2 + {}^aB^C c_3) + (A^T t_1 + B^T t_2 + {}^aB^T t_3)\right]\\
F_2 &= \mu\left[(A^C c_1 + B^C c_2 + {}^aB^C c_3) + (A^T t_1 + B^T t_2 + {}^aB^T t_3)\right]\\
F_3 &= -q_0 - h(\lambda^2+\mu^2)\left[(B^C c_1 + D^C c_2 + {}^aD^C c_3) + (B^T t_1 + D^T t_2 + {}^aD^T t_3)\right]\\
F_4 &= -q_0 - h(\lambda^2+\mu^2)\left[({}^sB^C c_1 + {}^sD^C c_2 + {}^sF^C c_3) + ({}^sB^T t_1 + {}^sD^T t_2 + {}^sF^T t_3)\right]
\end{aligned} \tag{24}$$

And

$$\begin{aligned}
&A^C = \int_{-h/2}^{h/2} \frac{E(z)}{1-\nu}\beta(z)dz,\ A^T = \int_{-h/2}^{h/2} \frac{E(z)}{1-\nu}\alpha(z)dz\\
&B^C = \int_{-h/2}^{h/2} \frac{E(z)}{1-\nu}\beta(z)\,\bar{z}\,dz,\ B^T = \int_{-h/2}^{h/2} \frac{E(z)}{1-\nu}\alpha(z)\,\bar{z}\,dz\\
&D^C = \int_{-h/2}^{h/2} \frac{E(z)}{1-\nu}\beta(z)\,\bar{z}^2\,dz,\ D^T = \int_{-h/2}^{h/2} \frac{E(z)}{1-\nu}\alpha(z)\,\bar{z}^2\,dz\\
&{}^aB^C = \int_{-h/2}^{h/2} \frac{E(z)}{1-\nu}\beta(z)\,\bar{\psi}(z)\,dz,\ {}^aB^T = \int_{-h/2}^{h/2} \frac{E(z)}{1-\nu}\alpha(z)\,\bar{\psi}(z)\,dz\\
&{}^aD^T = \int_{-h/2}^{h/2} \frac{E(z)}{1-\nu}\alpha(z)\,\bar{\psi}(z)\,\bar{z}\,dz,\ {}^aD^C = \int_{-h/2}^{h/2} \frac{E(z)}{1-\nu}\beta(z)\,\bar{\psi}(z)\,\bar{z}\,dz\\
&{}^sB^C = \int_{-h/2}^{h/2} \frac{E(z)}{1-\nu}\beta(z)\,\bar{f}(z)\,dz,\ {}^sB^T = \int_{-h/2}^{h/2} \frac{E(z)}{1-\nu}\alpha(z)\,\bar{f}(z)\,dz\\
&{}^sD^C = \int_{-h/2}^{h/2} \frac{E(z)}{1-\nu}\beta(z)\,\bar{f}(z)\,\bar{z}\,dz,\ {}^sD^T = \int_{-h/2}^{h/2} \frac{E(z)}{1-\nu}\alpha(z)\,\bar{f}(z)\,\bar{z}\,dz\\
&{}^sF^C = \int_{-h/2}^{h/2} \frac{E(z)}{1-\nu}\beta(z)\,\bar{f}(z)\,\bar{\psi}(z)\,dz,\ {}^sF^T = \int_{-h/2}^{h/2} \frac{E(z)}{1-\nu}\alpha(z)\,\bar{f}(z)\,\bar{\psi}(z)\,dz
\end{aligned} \tag{25}$$

With

$$\bar{z} = \frac{z}{h},\ \bar{f}(z) = \frac{f(z)}{h},\ \bar{\psi}(z) = \frac{1}{\pi}\sin\left(\frac{\pi z}{h}\right) \tag{26}$$

5. Numerical results and discussion

In order to validate the present refined theory, a combination of highly used components is used here in the functionally graded plate, where their physical and mechanical properties are determined in Table 1.

The dimensionless deflection and stresses are expressed in Eq. (27) by

$$\begin{aligned}
&\bar{w} = \frac{100D}{a^4 q_0} w\left(\frac{a}{2},\frac{b}{2}\right), \bar{\sigma}_x = \frac{1}{10^2 q_0}\sigma_x\left(\frac{a}{2},\frac{b}{2},\frac{h}{2}\right),\\
&\bar{\tau}_{xy} = \frac{1}{10q_0}\tau_{xy}\left(0,0,\frac{-h}{3}\right), \bar{\tau}_{xz} = -\frac{1}{10q_0}\tau_{xz}\left(0,\frac{b}{2},0\right),\\
&K_0 = \frac{a^4 K_w}{D}, J_O = \frac{a^2 J_1}{D} = \frac{b^2 J_2}{D}, D = \frac{h^3 E_c}{12(1-\nu^2)}
\end{aligned} \tag{27}$$

Table 1 Used material's properties

Material	Young's modulus E (GPa)	Poisson's ratio ν	Thermal expansion's coefficient α*(10^{-6}/°C)	Moisture concentration expansion β
Titanium, Ti-6Al-4V (Metal)	66.2	1/3	10.3	0.33
Zirconia, ZrO_2 (Ceramic)	117	1/3	7.11	0

Unless mentioned otherwise, it is considered that: $q_0 = 100GPa$, $a/h = 10$, $b/a = 3$, $p = 2$, $t_1 = t_2 = t_3 = 0$, $c_1 = c_2 = c_3 = 0$.

In this validation section, the convergence between the present model using four micromechanical models (Voigt, Reuss, LRVE and Mori-Tanaka) and the various high order shear deformation theories SHSDT (Sinusoidal High Order Shear Deformation Theory) (Zenkour 2006) and PHSDT (Polynomial High Order Shear Deformation Theory) (Reddy 2000) is very well demonstrated in Tables 2 to 4.

The Table 2 shows the elastic foundation parameters effect on the deflection and stresses of isotropic (ceramic) rectangular plate under mechanical load, it can be shown clearly that the variation of these stresses and deflection is dependent on the existence of the elastic foundations, where the presence of the Winkler and Pasternak elastic foundation parameters leads to the decreasing of the stresses and displacements of the isotropic plate.

The Tables 3 and 4 represents analogous results to those shown in Table 2 including, in these cases, the effect of the moisture and temperature concentrations for two cases: with only linear variation (as shown Table 3) and a combination of linear and non-linear variations (as shown in Table 4).

The found results are compared against those of PHSDT (Polynomial High Order Shear Deformation Theory) and SHSDT (Sinusoidal High Order Shear Deformation Theory). An excellent concordance is noticed between those of the present theory and other theories results for the different values of power law index "P" exhibited in these tables as well as for the various micromechanical models considered in this research, namely: Voigt's, Reuss's, LRVE's and Mori-Tanaka's

By taking into account the results unveiled in Tables 2 to 4, it should be noted that the number of variables in the present theory is reduced four unknowns, while this number rises to five unknowns in PHSDT (Polynomial High Order Shear Deformation Theory) and SHSDT (Sinusoidal High Order Shear Deformation Theory). From where, It can be easily concluded that the present theory (using the four micromechanical models) is not only precise but also relatively efficient and rather well-made in envisaging the hygro-thermo-mechanical Flexural behavior of functionally graded plates considering different micromechanical models and resting on elastic foundations.

Moreover, based on Fig. 2. the difference between the deflection results is clear for the case of mechanical loading, this caused by the description of the variation of the Young's modulus across the plate's thickness, where the Voigt's micromechanical model gives the highest values of Young's modulus (overestimating of Young's modulus) while Reuss's model gives its lowest value (underestimating of Young's modulus), with LRVE and Mori-Tanaka's models giving results between those of the two previous models (Voigt and Reuss). Additionally, under the effect of temperature and moisture, the difference in results become inconclusive for the reason that these micromechanical model's represent the variation of temperature and moisture through the plate's thickness in a different way of its representation of Young's modulus. This is due to the fact that Thermal expansion's and moisture concentration

Table 2 Effect of micromechanical model and elastic foundation on deflection and stresses variation of a rectangular ceramic plate under mechanical load

K_0	J_0	Micromechanical model	Theory	$\bar{w}$	$\bar{\sigma}_x$	$\bar{\tau}_{xy}$	$\bar{\tau}_{xz}$
0	0	Voigt	PHSDT (Reddy 2000)	0.85891	0.51545	0.72797	-0.42956
			SHSDT (Zenkour 2006)	0.85887	0.51362	0.72784	-0.44327
			Present	0.85889	0.51344	0.72797	-0.42829
		Reuss	Present	0.85889	0.51344	0.72797	-0.42829
		LRVE	Present	0.85889	0.51344	0.72797	-0.42829
		Mori-Tanaka	Present	0.85889	0.51344	0.72797	-0.42829
100	0	Voigt	PHSDT (Reddy 2000)	0.46206	0.27620	0.39162	-0.23109
			SHSDT (Zenkour 2006)	0.46205	0.27631	0.39158	-0.23847
			Present	0.46204	0.27621	0.39161	-0.23040
		Reuss	Present	0.46204	0.27621	0.39161	-0.23040
		LRVE	Present	0.46204	0.27621	0.39161	-0.23040
		Mori-Tanaka	Present	0.46204	0.27621	0.39161	-0.23040
0	100	Voigt	PHSDT (Reddy 2000)	0.08965	0.05358	0.07599	-0.04485
			SHSDT (Zenkour 2006)	0.08964	0.05361	0.07597	-0.04627
			Present	0.08964	0.05359	0.07598	-0.04470
		Reuss	Present	0.08964	0.05359	0.07598	-0.04470
		LRVE	Present	0.08964	0.05359	0.07598	-0.04470
		Mori-Tanaka	Present	0.08964	0.05359	0.07598	-0.04470
100	100	Voigt	PHSDT (Reddy 2000)	0.08228	0.04919	0.06972	-0.04116
			SHSDT (Zenkour 2006)	0.08227	0.04919	0.06972	-0.04246
			Present	0.08227	0.04918	0.06973	-0.04102
		Reuss	Present	0.08227	0.04918	0.06973	-0.04102
		LRVE	Present	0.08227	0.04918	0.06973	-0.04102
		Mori-Tanaka	Present	0.08227	0.04918	0.06973	-0.04102

Table 3 Effect of micromechanical model and elastic foundation on deflection and stresses variation of a rectangular FGM plate under linear hygro-thermo-mechanical load ($t_2 = 10$, $c_2 = 100$, $K_0 = J_0 = 100$).

P	Micromechanical model	Theory	$\bar{w}$	$\bar{\sigma}_x$	$\bar{\tau}_{xy}$	$\bar{\tau}_{xz}$
1	Voigt	PHSDT (Reddy 2000)	0.18504	-0.51450	0.15631	0.44545
		SHSDT (Zenkour 2006)	0.18504	-0.51476	0.15635	0.45984
		Present	0.18503	-0.51447	0.15630	0.44412
	Reuss	PHSDT* (Reddy 2000)	0.16625	-0.49486	0.09207	0.35092
		SHSDT* (Zenkour 2006)	0.16629	-0.49506	0.09214	0.36247
		Present	0.16627	-0.49486	0.09207	0.34986
	LRVE	PHSDT* (Reddy 2000)	0.18073	-0.51297	0.14321	0.42205
		SHSDT* (Zenkour 2006)	0.18074	-0.51324	0.14323	0.43534
		Present	0.18073	-0.51297	0.14318	0.42037
	Mori-Tanaka	PHSDT* (Reddy 2000)	0.17868	-0.51646	0.14388	0.40977
		SHSDT* (Zenkour 2006)	0.17868	-0.51671	0.14393	0.42308
		Present	0.17868	-0.51644	0.14387	0.40855
5	Voigt	PHSDT (Reddy 2000)	0.18696	-0.48940	0.12417	0.43754
		SHSDT (Zenkour 2006)	0.18694	-0.48967	0.12431	0.45322
		Present	0.18695	-0.48939	0.12415	0.43597
	Reuss	PHSDT* (Reddy 2000)	0.16551	-0.50314	0.10249	0.34117
		SHSDT* (Zenkour 2006)	0.16551	-0.50338	0.10257	0.35290
		Present	0.16551	-0.50313	0.10248	0.34010
	LRVE	PHSDT* (Reddy 2000)	0.18401	-0.50734	0.14126	0.42601
		SHSDT* (Zenkour 2006)	0.18401	-0.50761	0.14138	0.44108
		Present	0.18401	-0.50732	0.14124	0.42462
	Mori-Tanaka	PHSDT* (Reddy 2000)	0.18208	-0.51926	0.15232	0.41829
		SHSDT* (Zenkour 2006)	0.18208	-0.51953	0.15243	0.43300
		Present	0.18208	-0.51924	0.15230	0.41694

PHSDT*and SHSDT*: are results calculated using (Reddy 2000) and (Zenkour 2006) high order theories, respectively

coefficients are greater in the case of Titanium than those of Zirconia, conversely, Young's modulus of Zirconia is greater than Titanium's Young modulus. In another words, each micromechanical model underestimate one parameter and overestimate other and vis versa.

Table 4 Effect of micromechanical model and elastic foundation on deflection and stresses variation of a rectangul ar FGM plate under linear and nonlinear hygro-thermo-mechanical load ($t_2 = t_3 = 10$, $c_2 = c_3 = 100$, $K_0 = J_0 = 100$)

P	Micromechanical model	Theory	$\bar{w}$	$\bar{\sigma}_x$	$\bar{\tau}_{xy}$	$\bar{\tau}_{xz}$
1	Voigt	PHSDT (Reddy 2000)	0.26330	-0.86205	0.23762	0.82148
		SHSDT (Zenkour 2006)	0.26330	-0.86252	0.23772	0.84866
		Present	0.26330	-0.86201	0.23759	0.81900
	Reuss	PHSDT* (Reddy 2000)	0.22950	-0.82757	0.12500	0.64999
		SHSDT* (Zenkour 2006)	0.22950	-0.82795	0.12511	0.67179
		Present	0.22950	-0.82754	0.12499	0.64799
	LRVE	PHSDT* (Reddy 2000)	0.25535	-0.85922	0.21490	0.77866
		SHSDT* (Zenkour 2006)	0.25536	-0.85971	0.21494	0.80315
		Present	0.25536	-0.85923	0.21481	0.77493
	Mori-Tanaka	PHSDT* (Reddy 2000)	0.25151	-0.86565	0.21621	0.75508
		SHSDT* (Zenkour 2006)	0.25151	-0.86609	0.21632	0.78016
		Present	0.25151	-0.86562	0.21619	0.75277
5	Voigt	PHSDT (Reddy 2000)	0.26601	-0.81745	0.18459	0.80297
		SHSDT (Zenkour 2006)	0.26600	-0.81792	0.18486	0.83230
		Present	0.26601	-0.81741	0.18454	0.80020
	Reuss	PHSDT* (Reddy 2000)	0.22742	-0.84388	0.14756	0.62873
		SHSDT* (Zenkour 2006)	0.22742	-0.84429	0.14772	0.65079
		Present	0.22742	-0.84385	0.14753	0.62671
	LRVE	PHSDT* (Reddy (2000))	0.26067	-0.85042	0.21608	0.78192
		SHSDT* (Zenkour (2006))	0.26066	-0.85089	0.21634	0.81013
		Present	0.26067	-0.85038	0.21605	0.77934
	Mori-Tanaka	PHSDT* (Reddy 2000)	0.25722	-0.87198	0.23617	0.76813
		SHSDT* (Zenkour 2006)	0.25722	-0.87245	0.23641	0.79567
		Present	0.25723	-0.87194	0.23614	0.76561

PHSDT* and SHSDT*: are results calculated using (Reddy (2000)) and (Zenkour 2006) high order theories, respectively

Table 5 Effect of micromechanical model and side to thickness ratio a/h on deflection variation of a square FGM plate under linear and nonlinear hygro-thermo-mechanical load ($P = 2, t_2 = t_3 = 10$, $c_2 = c_3 = 100$)

K_0	J_0	Micromechanical model	Side to thickness ratio a/h			
			10	20	50	100
0	0	Voigt	1.79156	0.71642	0.41516	0.37211
		Reuss	1.54446	0.66141	0.41403	0.37868
		LRVE	1.76698	0.71349	0.41832	0.37614
		Mori-Tanaka	1.75365	0.71178	0.41988	0.37817
100	0	Voigt	1.29862	0.52553	0.30557	0.27402
		Reuss	1.11121	0.48185	0.30269	0.27699
		LRVE	1.27621	0.52167	0.30691	0.27611
		Mori-Tanaka	1.26439	0.51957	0.30756	0.27715
0	100	Voigt	0.21095	0.08769	0.05139	0.04613
		Reuss	0.17760	0.07916	0.05012	0.04592
		LRVE	0.20569	0.08640	0.05123	0.04614
		Mori-Tanaka	0.20301	0.08573	0.05115	0.04615
100	100	Voigt	0.20193	0.08396	0.04920	0.04417
		Reuss	0.16998	0.07578	0.04799	0.04396
		LRVE	0.19687	0.08272	0.04905	0.04418
		Mori-Tanaka	0.19431	0.08207	0.04897	0.04418

Table 5 demonstrates the effects of elastic foundation parameters versus side-to-thickness ratio on the dimensionless deflection of FGM square plate under hygro-thermo-mechanical loads using the present theory and four micromechanical models (Voigt, Reuss, LRVE and Mori-Tanaka). It can be clearly observed from this table and Fig. 2 that the deflection decreases with the rise of side-to-thickness ratio a/h for the different cases of loading exhibited in these figures, namely: mechanical in Fig. 2(a), hygro-mechanical in Fig. 2(b), thermomechanical in Fig. 2(c)and hygro-thermo-mechanical in Fig. 2(d). Furthermore, the inclusion of elastic foundation parameters

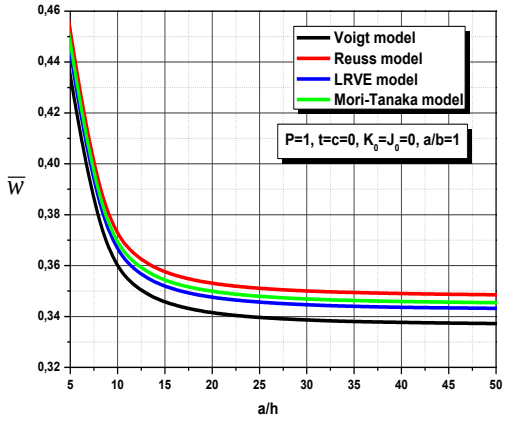

(a) Mechanical load

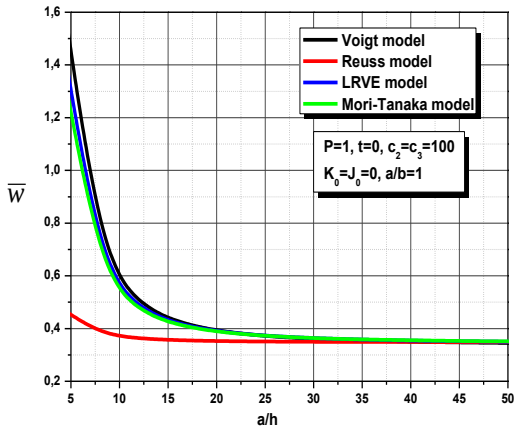

(b) Hygro-mechanical load

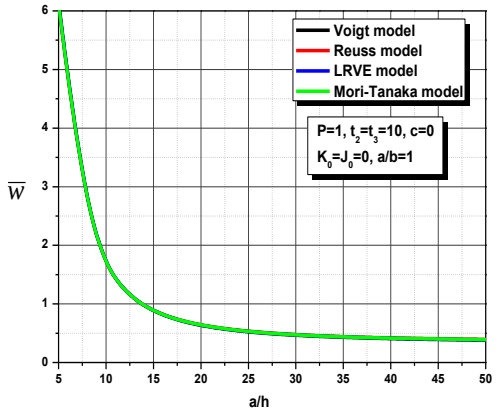

(c) Thermo-mechanical load

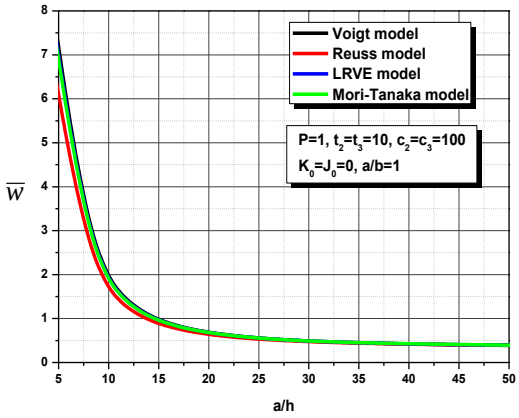

(d) Hygro-thermo-mechanical load

Fig. 2 Dimensionless deflection $\bar{w}$ of a square FGM plate under different types of loading

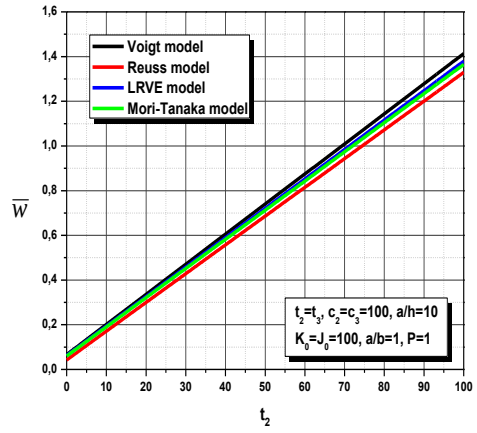

Fig. 3 Effect of temperature rise on deflection variation $\bar{w}$ of a square FGM plate on elastic foundations

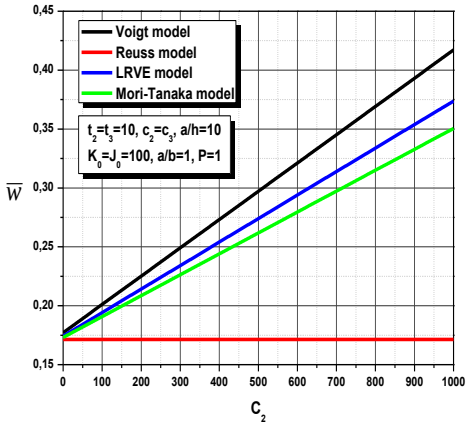

Fig. 4 Effect of moisture concentration rise on deflection variation $\bar{w}$ of a square FGM plate on elastic foundations

leads to a significant decrease of the central deflection, this can be easily explained by the fact that elastic foundations are in the opposite direction of the applied mechanical load, and contributes to the limitation of the deformation in the "z" axes.

Also, Figs .3-7 illustrate the influence the hygrothermal, elastic foundation and the aspect ratio (a/b) parameters on

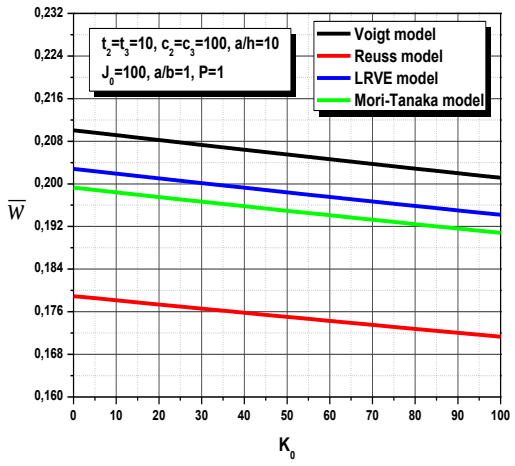

Fig. 5 Effect of Winkler elastic foundation deflection variation $\bar{w}$ of simply supported FGM square plate under hygro-thermo-mechanical load

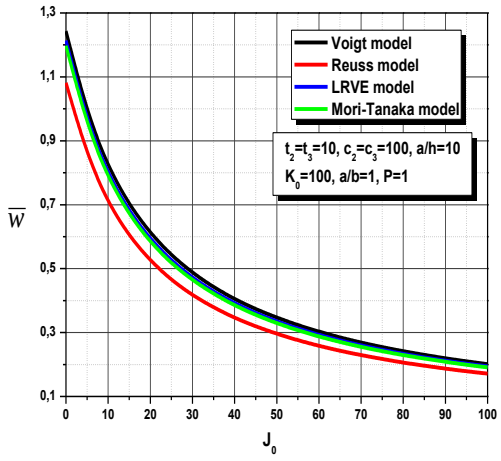

Fig. 6 Effect of Pasternak elastic foundation deflection variation $\bar{w}$ of simply supported FGM square plate under hygro-thermo-mechanical load

the central deflection variation of a the functionally graded plates. From where, it can be seen that this deformation is increased linearly by the linear increase of the temperature (t_2) and the moisture concentration (C_2), this mean that the existence of these two parameters add extra loading to the FGM plate. In addition, this displacement is decreased according to the increase of the elastic foundation parameters (K_0 and J_0) and the aspect ratio (a/b), from this, it can be concluded that these previous parameters stated in this paragraph are of a major importance in the study of flexural behavior of FGM plates.

The dimensionless longitudinal and transversal shear stresses ($\bar{\boldsymbol{\sigma}}_{\boldsymbol{x}}$, and $\bar{\boldsymbol{\tau}}_{\boldsymbol{xz}}$) variation across the thickness of a hygro-thermo-mechanically loaded FGM plate are well shown in Figs. 8 and 9. As exhibited Fig. 8, the longitudinal compressive stresses $\bar{\boldsymbol{\sigma}}_{\boldsymbol{x}}$, reaches its maximum value in the

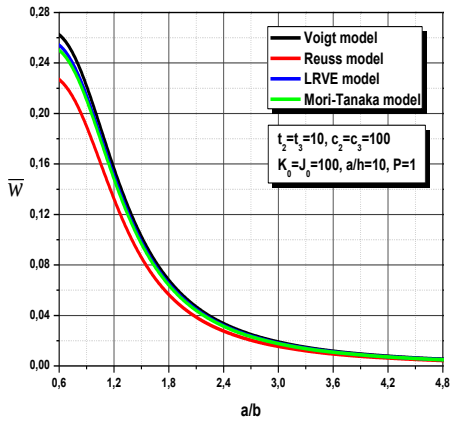

Fig. 7 Effect of aspect ratio a/b on deflection variation $\bar{w}$ of simply supported FGM square plate under hygro-thermo-mechanical load

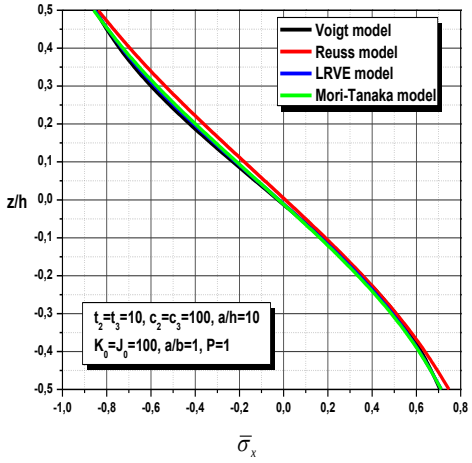

Fig. 8 Variation of normal stress $\bar{\sigma}_x$ through the thickness of a square FGM plate under hygro-thermo-mechanical load

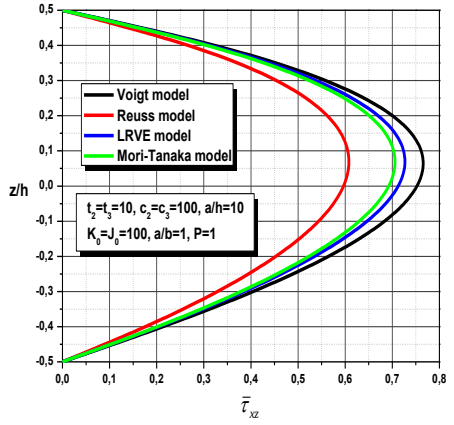

Fig. 9 Variation of shear stress $\bar{\tau}_{xz}$ through the thickness of a square FGM plate under hygro-thermo-mechanical load

top side of the plate, conversely the tensile one reaches its maximum value in the bottom side of the plate. Moreover, from Fig. 9 we can be undeniably emphasize the hypothesis of the present refined theory in terms of the parabolic variation of the shear stresses through the thickness and the nullity of these last at the top and bottom edges of the plate. Based on the previous results discussed in this section, for the case of mechanical loading, we can see that the Voigt micromechanical model underestimates the central deflection, while Reuss's model overestimates this displacement. On the contrary, for the case of hygro-thermo-mechanical loading, Reuss micromechanical model is the one who underestimates the central deflection and stresses also while Voigt's model overestimates them. In both cases, the LRVE and Mori-Tanaka micromechanical models give results close to the Voigt's model.

6. Conclusions

In this research paper, the flexural behavior of ceramic/metal functionally graded plates is examined using an efficient refined high order theory, the considered FGM plate is subjected to hygro-thermo-mechanical loading and supported by an elastic foundation. The validation of the present theory is very well established by comparing its results against those of other higher order theories (PHSDT and SHSDT). After validation, A parametric study was conducted to determine the main factors that affect significantly the bending behavior of the FGM plate in terms of deflection and stress, mainly: type of loading (mechanical, hygro-mechanical, thermo-mechanical and hygro-thermo-mechanical), plate geometrics (side to thickness ratio and aspect ratio), material's properties (Young's modulus variation), Elastic foundation (Winkler and Pasternak parameters), and most importantly, micromechanical models (Voigt, Reuss, LRVE and Mori-Tanaka).

The main conclusions drawn from this research are:

a. The presence of the Winkler and Pasternak elastic foundation parameters leads to significant decrease of the stresses and displacements of the FGM plate;
b. For all cases of loading exhibited here, the deflection decreases with the rise of side-to-thickness ratio a/h.
c. The deformation increases by the rise of the temperature and the moisture concentration in the FGM plate.
d. We must attach utmost importance to the choice of micromechanical models used for the study of flexural behavior of FGM plates under different loadings.

The extension of the present theory is also envisaged for general boundary conditions and plates of a more general shape. In conclusion, it can be said that the proposed theory is accurate and simple in solving the static behaviors of FGM plates.

References

Adim, B., Daouadji, T.H. and Abbes, B. (2016), "Buckling analysis of anti-symmetric cross-ply laminated composite plates under different boundary conditions", *Int. Appl. Mech.*, **52**(6), 661-676. https://doi.org/10.1007/s10778-016-0787-x.

Akbarzadeh, A.H., Abedini, A. and Chen, Z.T. (2015), "Effect of micromechanical models on structural responses of functionally graded plates", *Compos. Struct*., **119**, 598-609. https://doi.org/10.1016/j.compstruct.2014.09.031.

Amari, A. and Maktoof, M.A.J. (2023), "On the response of the sandwich shell subjected to thermo-mechanical shock loading", *Waves in Random and Complex Media*, 1-21. https://doi.org/10.1080/17455030.2023.2194449.

Bagheri, H., Eslami, M.R. and Kiani, Y. (2023), "Geometrically nonlinear response of FGM joined conical–conical shells subjected to thermal shock", *Thin-Walled Struct.*, **182**, 110171. https://doi.org/10.1016/j.tws.2022.110171.

Bagheri, H., Kiani, Y. and Eslami, M.R. (2021), "Free vibration of FGM conical–spherical shells", *Thin-Walled Struct.,* **160**, 107387. https://doi.org/10.1016/j.tws.2020.107387.

Cao, J., Du, J., Zhang, H., He, H., Bao, C. and Liu, Y. (2024), "Mechanical properties of multi-bolted Glulam connection with slotted-in steel plates", *Constr. Build. Mater.*, **433**, 136608. https://doi.org/10.1016/j.conbuildmat.2024.136608.

Daouadji, T.H. and Adim, B. (2016), "An analytical approach for buckling of functionally graded plates", *Adv. Mater. Res.*, **5**(3), 141-169. https://doi.org/10.12989/amr.2016.5.3.141.

Daouadji, T.H., Benferhat, R. and Adim, B. (2016), "Bending analysis of an imperfect advanced composite plates resting on the elastic foundations", *Coupled Syst. Mech.*, **5**(3), 269-283. https://doi.org/10.12989/csm.2016.5.3.269.

Daouadji, T.H., Chedad, A. and Adim, B. (2016), "Interfacial stresses in RC beam bonded with a functionally graded material plate", *Struct. Eng. Mech.*, **60**(4), 693-705. https://doi.org/10.12989/sem.2016.60.4.693.

Gao, Q., Ding, Z. and Liao, W.H. (2022), "Effective elastic properties of irregular auxetic structures", *Compos. Struct.*, **287**, 115269. https://doi.org/10.1016/j.compstruct.2022.115269.

Gasik, M.M. (1998), "Micromechanical modelling of functionally graded materials", *Comput. Mater. Sci.*, **13**(1-3), 42-55. https://doi.org/10.1016/S0927-0256(98)00044-5.

Ghiasian, S.E., Kiani, Y. and Eslami, M.R. (2013), "Dynamic buckling of suddenly heated or compressed FGM beams resting on nonlinear elastic foundation", *Compos. Struct.,* **106**, 225-234. https://doi.org/10.1016/j.compstruct.2013.06.001.

Gupta, A., Talha, M. and Chaudhari, V.K. (2016), "Natural frequency of functionally graded plates resting on elastic foundation using finite element method", *Procedia Technol.*, **23**, 163-170. https://doi.org/10.1016/j.protcy.2016.03.013.

Hachemi, H., Kaci, A., Houari, M.S.A., Bourada, M., Tounsi, A. and Mahmoud, S.R. (2017), "A new simple three-unknown shear deformation theory for bending analysis of FG plates resting on elastic foundations", *Steel Compos. Struct*., **25**(6), 717-726. https://doi.org/10.12989/scs.2017.25.6.717.

Kaddari, M., Kaci, A., Bousahla, A.A., Tounsi, A., Bourada, F., Bedia, E.A. and Al-Osta, M.A. (2020), "A study on the structural behaviour of functionally graded porous plates on elastic foundation using a new quasi-3D model: bending and free vibration analysis", *Comput. Concrete*, **25**(1), 37-57. https://doi.org/10.12989/cac.2020.25.1.037.

Kiani, Y. and Eslami, M.R. (2014), "Geometrically non-linear rapid heating of temperature-dependent circular FGM plates", *J. Therm. Stresses,* **37**(12), 1495-1518. http://dx.doi.org/10.1080/01495739.2014.937259.

Kiani, Y. and Eslami, M.R. (2015), "Thermal postbuckling of imperfect circular functionally graded material plates: examination of Voigt, Mori–Tanaka, and self-consistent schemes", *J. Press. Vess. Technol.,* **137**(2), 021201. https://doi.org/10.1115/1.4026993.

Kiani, Y., Sadighi, M. and Eslami, M.R. (2013), "Dynamic

analysis and active control of smart doubly curved FGM panels", *Compos. Struct.*, **102**, 205-216. http://dx.doi.org/10.1016/j.compstruct.2013.02.031.

Kitipornchai, S., Yang, J. and Liew, K.M. (2006), "Random vibration of the functionally graded laminates in thermal environments", *Comput. Method. Appl. Mech Eng.*, **195**(9-12), 1075-1095. https://doi.org/10.1016/j.cma.2005.01.016.

Liu, K., Zong, S., Li, Y., Wang, Z., Hu, Z. and Wang, Z. (2022), "Structural response of the U-type corrugated core sandwich panel used in ship structures under the lateral quasi-static compression load", *Mar. Struct.*, **84**, 103198. https://doi.org/10.1016/j.marstruc.2022.103198.

Mori, T. and Tanaka, K. (1973), "Average stress in matrix and average elastic energy of materials with misfitting inclusions", *Acta Metallurgica*, **21**(5), 571-574. https://doi.org/10.1016/0001-6160(73)90064-3.

Mudhaffar, I.M., Tounsi, A., Chikh, A., Al-Osta, M.A., Al-Zahrani, M.M. and Al-Dulaijan, S.U. (2021), "Hygro-thermo-mechanical bending behavior of advanced functionally graded ceramic metal plate resting on a viscoelastic foundation", *Structures*, **33**, 2177-2189. https://doi.org/10.1016/j.istruc.2021.05.090.

Nemati, A.R. and Mahmoodabadi, M.J. (2020), "Effect of micromechanical models on stability of functionally graded conical panels resting on Winkler–Pasternak foundation in various thermal environments", *Arch. Appl. Mech.*, **90**(5), 883-915. https://doi.org/10.1007/s00419-019-01646-6.

Nguyen, N.D., Nguyen, T.N., Nguyen, T.K. and Vo, T.P. (2023), "A Legendre-Ritz solution for bending, buckling and free vibration behaviours of porous beams resting on the elastic foundation". *Structures*, **50**, 1934-1950. https://doi.org/10.1016/j.istruc.2023.03.018.

Parida, S. and Mohanty, S.C. (2018), "Free vibration and buckling analysis of functionally graded plates resting on elastic foundation using higher order theory", *Int. J. Struct. Stab. Dyn.*, **18**(4), 1850049. https://doi.org/10.1142/S0219455418500499.

Reddy, J.N. (2000), "Analysis of functionally graded plates", *Int. J. Numer. Meth. Eng.*, **47**, 663-684. https://doi.org/10.1002/(SICI)1097-0207(20000110/30)47:1/3<663::AID-NME787>3.0.CO;2-8.

Sadowski, T., Birsan, M. and Pietras, D. (2015), "Multilayered and FGM structural elements under mechanical and thermal loads. Part I: Comparison of finite elements and analytical models", *Arch. Civil Mech. Eng.*, **15**(4), 1180-1192. https://doi.org/10.1016/j.acme.2014.09.004.

Shahsavari, D. and Karami, B. (2022), "Assessment of Reuss, Tamura, and LRVE models for vibration analysis of functionally graded nanoplates", *Arch. Civil Mech. Eng.*, **22**(2), 92. https://doi.org/10.1007/s43452-022-00409-5.

Shariyat, M., Jahanshahi, S. and Rahimi, H. (2019), "Nonlinear Hermitian generalized hygrothermoelastic stress and wave propagation analyses of thick FGM spheres exhibiting temperature, moisture, and strain-rate material dependencies", *Compos. Struct.*, **229**, 111364. https://doi.org/10.1016/j.compstruct.2019.111364.

Sharma, P. and Singh, R. (2019), "Investigation on modal behaviour of FGM annular plate under hygrothermal effect", *IOP conference series: materials science and engineering*, **624**(1), 012001. https://doi.org/10.1088/1757-899X/624/1/012001.

Sobhy, M. (2016), "An accurate shear deformation theory for vibration and buckling of FGM sandwich plates in hygrothermal environment", *Int. J. Mech. Sci.*, **110**, 62-77. https://doi.org/10.1016/j.ijmecsci.2016.03.003.

Soltani, K., Bessaim, A., Houari, M.S.A., Kaci, A., Benguediab, M., Tounsi, A. and Alhodaly, M.S. (2019), "A novel hyperbolic shear deformation theory for the mechanical buckling analysis of advanced composite plates resting on elastic foundations", *Steel Compos. Struct.*, **30**(1), 13-29. https://doi.org/10.12989/scs.2019.30.1.013.

Tounsi, A., Bousahla, A.A., Tahir, S.I., Mostefa, A.H., Bourada, F., Al-Osta, M.A. and Tounsi, A. (2023), "Influences of different boundary conditions and hygro-thermal environment on the free vibration responses of FGM sandwich plates resting on viscoelastic foundation", *Int. J. Struct. Stab. Dyn.*, 2450117. https://doi.org/10.1142/S0219455424501177.

Wang, Y. and Sigmund, O. (2023), "Multi-material topology optimization for maximizing structural stability under thermo-mechanical loading", *Comput. Method. Appl. M.*, **407**, 115938. https://doi.org/10.1016/j.cma.2023.115938.

Zaidi, M., Joshi, K.K., Shukla, A. and Cherinet, B. (2021), "A review of the various modelling schemes of unidirectional functionally graded material structures", *AIP Conference Proceedings, AIP Publishing*, **2341**(1). https://doi.org/10.1063/5.0050306.

Zenkour, A.M. (2006), "Generalized shear deformation theory for bending analysis of functionally graded plates", *Appl. Math. Modell.*, **30**(1), 67-84. https://doi.org/10.1016/j.apm.2005.03.009.

Zhang, C., Khorshidi, H., Najafi, E. and Ghasemi, M. (2023), "Fresh, mechanical and microstructural properties of alkali-activated composites incorporating nanomaterials: A comprehensive review", *J. Cleaner Product.*, **384**, 135390. https://doi.org/10.1016/j.jclepro.2022.135390.

Zhang, H., Liu, H. and Kuai, H. (2024), "Stress intensity factor analysis for multiple cracks in orthotropic steel decks rib-to-floorbeam weld details under vehicles loading", *Eng. Fail. Anal.*, **164**, 108705. https://doi.org/10.1016/j.engfailanal.2024.108705.

Zhang, L., Lin, Q., Chen, F., Zhang, Y. and Yin, H. (2020), "Micromechanical modeling and experimental characterization for the elastoplastic behavior of a functionally graded material", *Int. J Solids Struct.*, **206**, 370-382. https://doi.org/10.1016/j.ijsolstr.2020.09.010.

Zuiker, J.R. (1995), "Functionally graded materials: choice of micromechanics model and limitations in property variation", *Compos. Eng.*, **5**(7), 807-819. https://doi.org/10.1016/0961-9526(95)00031-H.

JS